

Green tea catechin prevents oxidative stress-regulated autophagy and apoptosis signaling, and inhibits tenderness in postmortem bovine *longissimus thoracis et lumborum* muscle

Xijin Zhu, Aixia Li, Nan Sun, Ling Han^{*}, Qunli Yu^{*}

College of Food Science and Engineering, Gansu Agricultural University, Lanzhou, Gansu 730070, PR China

ARTICLE INFO

Keywords:

Green tea catechin
Oxidative stress
Autophagy
Apoptosis
Tenderization
Bovine

ABSTRACT

Although green tea catechin has been reported to be an antioxidant and preservative in meat, the extent to which it affects the tenderization of bovine muscle remains largely unknown. This study seeks to evaluate the effect of catechin on the interplay between apoptosis and autophagy, and subsequently, the development of bovine muscle tenderness. The results indicate that catechin significantly alleviated oxidative stress. A concomitant reduction of autophagic markers LC3-II/LC3-I ratio, Beclin-1, and Atg7 levels were caused by catechin. Besides, aforementioned autophagy inhibition was further augmented by PI3K/Akt/mTOR activation. Additionally, catechin protected against mitochondrial dysfunction and inhibited mitochondria-dependent caspase apoptosis pathway. Furthermore, there was a reciprocal inhibition between autophagy and apoptosis. Ultimately, tenderness at 24 and 120 h, an increase in the gap between muscle fiber bundles, and disintegration of myofibrillar architectures were all inhibited by catechin. Therefore, despite alleviating oxidative stress, catechin may hamper tenderization pattern of postmortem bovine muscle.

1. Introduction

Among all meat characteristics, tenderness is widely regarded as the most organoleptic trait that determines consumers' purchase intention (Zhang et al., 2018, Zhang et al., 2018). Nevertheless, tenderness is a highly variable trait, and relies on many factors and mechanisms during the life of the animal. Therefore, the tissue changes occurring after the animal's death remain incompletely understood.

In postmortem muscle, an abrupt cessation of blood circulation and oxygen results in a dramatic energy supply reduction. This, in turn, impairs the mitochondrial electron transport chain, which alters reactive oxygen species (ROS) production and resultant oxidative stress (Lana & Zolla, 2015). The overwhelming oxidative stress may ultimately turn over damaged organelles within a cell through autophagy, alternatively, lead to the destruction of the cell through programmed cell death (PCD) pathway induction under the condition that cell viability cannot be sustained (García-Macia et al., 2014).

Apoptosis, previously referred to as type I PCD, is a regulated form of cell death characterized at morphological, biochemical, and molecular levels. Thus far, apoptosis is considered to have the most potential process of cell death in postmortem muscle, serving as the first stage of

postmortem tenderization. Specifically, apoptosis and its effects initiate and facilitate the proteolytic degradation of crucial myofibrillar, thereby contributing to the transformation of muscle into meat (Zhang et al., 2018, Zhang et al., 2018). The process can be regulated via two main routes regarding mitochondria (the intrinsic pathway) and death-receptor (the extrinsic pathway; Herrera-Mendez et al., 2006). Among them, classical mitochondrion-mediated apoptosis is believed as the principal mechanism during postmortem aging (Wang et al., 2018a, Wang et al., 2018b). Oxidative stress has been established as a key event in apoptotic cell models, as it facilitates the apoptotic program via hitting the membrane permeability transition pore (MPTP), and mitochondrial swelling coupled with the cytochrome c leakage into the cytosol, and ultimately promoting the apoptotic cascade (Wang et al., 2018a, Wang et al., 2018b). Alternatively, in response to excessive oxidative stress, autophagy (type II PCD), as a main cellular defense mechanism, is triggered in which cytoplasmic proteins or whole organelles are self-digested by lysosomes. Given this, postmortem aging appears to accomplish characteristics of apoptosis and autophagy due to the central feature of oxidative stress. Notably, some studies witnessed that autophagy appeared in the early postmortem muscle, and autophagic biomarkers LC3 and Beclin-1 are highly expressed (García-Macia

^{*} Corresponding authors.

E-mail addresses: hlsciggyxz@126.com (L. Han), yuqunlisciscii@126.com (Q. Yu).

<https://doi.org/10.1016/j.fochx.2023.100758>

Received 22 November 2022; Received in revised form 11 June 2023; Accepted 15 June 2023

Available online 22 June 2023

2590-1575/© 2023 The Authors. Published by Elsevier Ltd. This is an open access article under the CC BY-NC-ND license (<http://creativecommons.org/licenses/by-nc-nd/4.0/>).

et al., 2014). Others also evidenced the occurrence of both apoptosis and autophagy in broiler thigh muscle under oxidative stress (Yan et al., 2022). However, to our knowledge, the relationship between autophagy and tenderness presents ubiquitously uncertainties in all other kinds of aging meat, and little information is available regarding the autophagy and apoptosis combined in the postmortem muscle.

Recently, natural antioxidants are of great interest for their benefits in health promotion and disease-preventing effects. Among these, green tea catechin, a flavonoid with potent free radical scavenging and antioxidant properties, has emerged as a promising candidate. Its cost-effectiveness compared to other natural sources of antioxidants has made it a highly valued component in the food industry (Namal Senanayake, 2013). The efficacy of catechin as an antioxidant or preservative has been known in the field of meat science. Dietary catechin supplementation improves the antioxidant activity of ducks (Tian & Huang, 2019) and lambs (Zhong et al., 2015). In recent years, catechin presents a growing concern for the extensive spectrum of positive health impacts on diverse diseases through the regulatory effect on apoptosis and autophagy. However, there is much debate regarding the function of catechin in cell death. It has been suggested that catechin reduces apoptosis by restraining oxidative stress (Chen et al., 2016). In human melanoma skin A375 cells, catechin induces apoptosis via the mitochondrial pathway while impeding autophagy, with both processes operating independently of one another (Du et al., 2022). Nevertheless, divergent perspectives exist, as autophagy inhibition promotes EGCG-mediated apoptosis in papillary thyroid cancer cells (Bu et al., 2021). The influence of catechin on cell death may differ depending on cell type, signaling pathways, active constituents, etc. Nevertheless, the precise role of catechin in promoting or inhibiting apoptosis and autophagy, as well as the potential interplay between these processes and their subsequent effects on postmortem bovine muscle tenderization, remains unclear due to insufficient evidence.

The aforementioned evidence clearly outlines the tight relationship between oxidative stress and apoptosis and autophagy. Furthermore, the state of oxidative stress upon hypoxia in postmortem muscle opens speculation that the probable biochemical behaviors of catechin on the postmortem muscle. Therefore, the present research aims to explore the effect of catechin on the tenderness of postmortem bovine muscle, with a particular focus on the mechanisms involved in apoptotic and autophagy processes. Our research may contribute to a fundamental investigation of the muscle-to-meat conversion/anti-oxidative effect duality of catechin with both a scientific and practical interest.

2. Materials and methods

2.1. Sample preparation

All procedures and protocols involving animals were in compliance with the Animal Ethics Procedures and Guidelines of the People's Republic of China and approved by Gansu Agricultural University Institutional Animal Care and Use Committee and Ethics Committee (approved ID: 2012-2-159).

Animals were raised and managed under the same specific pathogen-free conditions. A total of six crossbred bulls (Simmental \times local yellow cattle) with identical genetic backgrounds, weighing between 450–500 kg and approximately 2.5 years old were obtained. After the rest period and being declared healthy, animals were humanely slaughtered in a commercial abattoir (Kang Mei Co. Ltd, Gansu, China). The *Longissimus thoracis et lumborum* (LTL) muscle was expeditiously excised at the cutting line within 20 min of exsanguination and cut into 2.54-cm steaks instantly. Among these, two steaks were randomized and assigned as 0 h samples. The remaining steaks were divided into seven groups and subjected to various treatments, including injection with 0.9% normal saline (control), (+)-catechin from green tea (purity \geq 98% (HPLC), 300 μ M), catechin (300 μ M) + 740Y-P (a PI3K/Akt/mTOR signaling linkage agonist; 150 μ M), catechin (300 μ M) + 7407-P (150 μ M) + Z-VAD-FMK

(Z-VAD; a specific apoptosis inhibitor; 100 μ M), catechin (300 μ M) + H₂O₂ (an inducer of oxidative stress; 20 mM), catechin (300 μ M) + N-acetyl cysteine (NAC; a ROS inhibitor; 20 mM), and catechin (300 μ M) + NAC (20 mM) + 3-MA (an autophagy inhibitor; 10 mM) at the ratio 10:1 (w/v) (meat/buffer) in 1 min intervals. All the inhibitors and activators were purchased from Sigma (Sigma-Aldrich, St. Louis, MO). Preliminary experiments were performed to establish the optimal concentrations for each agonist and inhibitor. The needle was penetrated vertically through the top, bottom, and side of the slice to a depth of half the steak, followed by a careful massage for 35 sec upon withdrawing the needles to ensure even distribution of the buffers. Samples were incubated under vacuum conditions for 24, 72, and 120 h at 4 °C. Following each aging period, one steak from different treatments was subjected to apoptotic nucleus assay, Warner-Bratzler shear force (WBSF) assay, hematoxylin-eosin (HE) staining and scanning electron microscopy (SEM) assay, and the other were promptly frozen in liquid nitrogen and kept at –80 °C for further biochemical analyses.

2.2. Mitochondrial extraction

The mitochondrial isolation procedure was adapted from that of Li et al. (1999) with minor modifications. Minced muscles were homogenized in a 10-fold volume of buffer A consisting of 220 mM mannitol, 70 mM sucrose, 2.0 mM EDTA, 5.0 mM 4-morpholinepropanesulfonic acid, and 0.5% bovine serum albumin (BSA) (pH = 7.4) on ice. The homogenate was subjected to centrifugation at 1,000 \times g for 10 min (4 °C), and this process was repeated twice. The resulting supernatant was harvested, pooled, and again centrifuged at 8,000 \times g for 20 min (4 °C) in buffer B which was prepared by diluting it 7.5-fold with PBS-free buffer A, pH = 7.4. The resultant pellet fraction was used as the mitochondrial fraction while the supernatant was used as the cytosolic fraction.

2.3. ROS levels

The determination of intracellular ROS levels was conducted using 2', 7'-dichloro-dihydro-fluorescein diacetate (DCFH-DA; Zhang et al., 2020). To prepare the sample, minced muscle (0.5 g) was homogenized with a sixfold volume of buffer containing 10 mM Tris-HCl, 10 mM sucrose, 0.1 mM EDTA-2Na, and 0.8% [w/v] NaCl, pH 7.4). The homogenate was then centrifuged at 3,000 \times g (15 min), and the supernatant was collected. The protein concentration was quantified using a BCA assay kit (Catalog No. 23225; Pierce Biotechnology, Inc., Rockford, IL). Subsequently, 100 μ L of supernatant was subjected to incubation with 10 μ M DCFH-DA at equal volumes for 25 min at 37 °C in the dark. The fluorescence intensity was measured with an excitation wavelength of 488 nm and an emission wavelength of 525 nm using a fluorescence spectrophotometer (Shimadzu RF 5301, Kyoto, Japan). ROS changes were reported as fluorescence per mg of protein.

2.4. Analysis of antioxidant enzyme activity

The superoxide dismutase (SOD) and glutathione peroxidase (GSH-Px) activities were assayed referred to Chen et al. (2010). For the preparation of the muscle samples, tissues were homogenized in ice-cold phosphate buffered saline (PBS) to prepare 10% homogenate, then centrifuged (4 °C, 2000 \times g, 10 min), and the supernatants were obtained for SOD and GSH-Px activity assays. SOD activity was determined based on the inhibition of the reaction of hydroxylamine with the superoxide radical anion generated in the xanthine–xanthine oxidase system using a SOD commercial kit (Catalog No. A001; Nanjing Jian-Cheng Bioengineering Institute, Nanjing, China). Briefly, the supernatant (0.05 mL) collected was added to a 96-well plate and mixed with a SOD assay mixture, and incubated at 37 °C for 40 min. After incubation, color developer (2.0 mL) was added to the mixture and incubated for 10 min. Finally, the absorbance was measured at 550 nm and the activity was presented as units per mg of protein. GSH-Px promotes the reaction

of H₂O₂ with reduced glutathione to produce H₂O and oxidized glutathione (GSSG). The sulfhydryl group of GSH reacts with 5, 5'-dithiobis-(2-nitrobenzoic) acid (DTNB) to produce the stable yellow-colored 5-thio-2-nitrobenzoic acid (TNB) with a maximum absorbance at 412 nm. The activity was detected by a GSH-Px assay kit from Jiancheng Bioengineering Institute (Catalog No. A005) following the manufacturer's instructions. Glutathione was used to complete the reaction and H₂O₂ was used as the substrate of glutathione. The supernatants obtained were incubated with the working reagents included in the kits. After centrifuging at 4,000 × g, 1.0 mL of the supernatant was used for color development. Finally, the absorbance was read at 412 nm using an ultraviolet (UV) spectrophotometer (UV2550, Shimadzu, Kyoto, Japan). Enzyme activity can be decreased by negative feedback from the excess substrate and expressed as units per mg protein.

Glutathione peroxidase 4 (GPX4) level assay was performed referring to the method from Liu et al. (2023). A commercial enzyme-linked immunosorbent assay (ELISA) kit for the detection of GPX4 (Catalog No. H545-1; Nanjing Jiancheng Bioengineering Institute; Nanjing; China) was performed following the manufacturer's instructions. Briefly, the muscle samples were homogenized in ice-cold phosphate-buffered saline (PBS) with a weight (g)/volume (mL) ratio of 1:9 using a glass manual homogenizer. Subsequently, the resulting mixture was centrifuged at 3,000 × g at 4 °C for 10 min. The ELISA kits were allowed to equilibrate to room temperature for a duration of 30 min prior to commencing the assay, and standard wells and test sample wells were set. Standard wells were added to different concentrations of standard 50 μL, whereas the sample wells were initially administered 10 μL of the sample to be tested, followed by 40 μL of the sample diluent. With the exception of the blank wells, 100 μL horseradish peroxidase (HRP) labeled detection antibody was added. Afterward, the plate was incubated for 60 min at 37 °C. Subsequently, the liquid in each well was discarded, and the wells were shaken to dry, each well was washed with the diluted washing solution, which was repeated 5 times. Subsequently, 50 μL of Substrate A and B were introduced to each plate, followed by an incubation for 15 min at 37 °C in the dark. Finally, 50 μL of stopping solution was added to stop the reaction, and the OD₄₅₀ values were obtained using a microplate reader.

2.5. Measurement of lipid peroxidation

The degree of lipid peroxidation was assayed with a thiobarbituric acid (TBA) reaction referred to by Brenselová et al. (2015).

2.6. Western blot

Western blot assays were conducted according to the procedures of Du et al. (2021). Tissue homogenate was obtained through muscle samples (1.0 g) homogenized in a 9 mL buffer (0.01 M sodium phosphate and 2% SDS, pH = 7.4). The homogenates were centrifuged at 10,000 × g for 15 min and the supernatant was collected. For immunoblotting, proteins were separated by sodium dodecyl sulfate–polyacrylamide gel electrophoresis (SDS-PAGE) using Mini-PROTEAN® Tetra System (Bio-Rad Laboratories, Hercules, CA, USA) with a 12% (Bcl-2, Bax, Atg7, Beclin-1, and LC3, PI3K and Akt) and 8% (mTOR) separation gels and stacking gel. In specific, after heat denaturation in loading buffer at 95 °C for 5 min, and protein samples were loaded (20 μg samples per lane). Gels were run at 80 V constant voltage for approximately 1.5 h until the front reached the end of the gel at room temperature. Then, the proteins were transferred to PVDF membranes (Catalog No. ISEQ00010; Millipore Sigma). The PVDF membrane was soaked in methyl alcohol for 2–3 min and then the membrane and filter paper were incubated in an ice-cold transfer buffer. A 'sandwich' was mounted in the following order: filter paper, membrane, gel, and filter paper. After gel transfer, the membranes were blocked with a blocking buffer for 1 h under gentle shaking. After that, membranes were incubated with the following primary antibodies overnight at 4 °C: anti-PI3K (1:1,000 dilution; Catalog

No. 4249; Cell Signaling Technology), anti-p-PI3K (1:1,000 dilution; Catalog No. 17366; Cell Signaling Technology), anti-Akt (1:1,000 dilution; Catalog No. 9272; Cell Signaling Technology), anti-p-Akt (1:1,000 dilution; Catalog No. 4060; Cell Signaling Technology), Atg7 (1:1,000 dilution; Catalog No. 8558; Cell Signaling Technology), and anti-GAPDH (1:1,000 dilution; Catalog No. 2118; Cell Signaling Technology), anti-mTOR (1:1,000 dilution; Catalog No. 2972; Cell Signaling Technology), anti-p-mTOR (1:1,000 dilution; Catalog No. 2971; Cell Signaling Technology), anti-Bax (1:1,000 dilution; Catalog No. sc-493; Santa Cruz), anti-Bcl-2 (1:1,000 dilution; Catalog No. sc-492; Santa Cruz), LC3 (1:1,000 dilution; Catalog No. 14600–1-AP, Proteintech Group, Inc.), Beclin-1 (1:1,000 dilution; Catalog No. 3738; Cell Signaling Technology). After washing three times with TBST, they were incubated with an HRP-conjugated secondary antibody (1:3,000 dilution; Catalog No. A9169; Sigma-Aldrich) for 1 h and then washed again three times. Bands were visualized by an ECL reagent (Catalog No. RPN2106; Amersham Bioscience, Saclay, France) using a ChemiDoc MP imaging system (170-8280, Bio-Rad, Hercules, CA, USA). Densitometric analysis of immunoblots was conducted with Image J software (NIH, Bethesda, MD) allowing normalization with GAPDH.

2.7. Apoptotic nucleus assays

The apoptosis assay was conducted with the TdT-mediated dUTP Nick End Labeling (TUNEL) method referred to by Zhang et al. (2017). In brief, muscle specimens on the slides were serially fixed with 4% paraformaldehyde, followed by washing in PBS for 5 min × 3/time and blocking with 3% H₂O₂ to quench endogenous peroxidase activity and washed with PBS 3 times. Afterward, samples were permeabilized with 0.1% Triton X-100 and 0.1% sodium nitrate, and blocked with 5% normal goat serum for 30 min. TUNEL detective mixture was pipetted on the slides followed by incubation at 37 °C for 60 min in the dark. The TUNEL reaction mixture was prepared by the addition of 50 μL of TdT and 450 μL of fluorescein-labeled dUTP solution. To ensure the specificity of the TUNEL assay in each experiment, both negative and positive control were confirmed. The negative control involved the omission of the TdT enzyme in the TUNEL reaction mixture, while the positive control included sections treated with 5.1 U/mL DNase I for 10 min prior to TUNEL staining. TUNEL positive cells were observed and photographed with a fluorescence microscope (BX43; Olympus, Tokyo, Japan). The nuclei were counterstained with 4',6-diamidino-2-phenylindole (DAPI; Catalog No. AR1177; Boster Bioengineering Co., Ltd., Wuhan, China) and exhibited a blue fluorescence, while apoptotic cells were green. The positive nucleus was measured in at least ten representative independent microscopic fields (×200). The apoptosis rate was defined as the positive nuclei number/DAPI-positive nuclei.

2.8. Measurement of MPTP opening

MPTP opening was evaluated by measuring the variations in absorbance (Wang et al., 2018a, Wang et al., 2018b). Specifically, isolated mitochondria pellets were suspended in a 3.0 mL medium consisting of 230 mM mannitol, 70 mM sucrose, and 3.0 mM HEPES, pH = 7.4, resulting in a protein concentration of 0.3 mg/mL. Then, a mixture of 1.0 mL of the mitochondrial suspension and 3.0 mL of the test medium was transferred to a quartz cuvette and the absorbance was measured at a wavelength of 540 nm.

2.9. Mitochondrial membrane potential (MMP)

The determination of mitochondrial membrane potential was conducted as described previously (Wang et al., 2018a, Wang et al., 2018b). Specifically, 5,5',6,6'-tetrachloro-1,1',3,3'-tetraethyl-benzimidazole carbon iodide (JC-1), a dual-emission mitochondrial dye, was employed using a commercially available kit according to the manufacturer's instructions (Catalog No. C2006; Beyotime, Beijing, China). In brief, the

prepared JC-1 staining working solution was subjected to a 5-fold dilution with JC-1 staining buffer. Subsequently, 0.9 mL of the diluted JC-1 staining working solution was introduced to 0.1 mL of purified mitochondria obtained in section 2.2. Subsequently, the fluorescence intensity was measured with the follow parameters: excitation wavelength of 490 nm and an emission wavelength of 530 nm for JC-1 monomers and an excitation wavelength of 525 nm and an emission wavelength of 590 nm for JC-1 aggregates by a fluorescence spectrophotometer. The ratio of red/green fluorescence represented mitochondrial membrane potential.

2.10. Caspases activities assay

The caspases activities were detected according to Cao et al. (2013) with few modifications. Muscle samples (150 mg) were homogenized in 0.5 mL of lyses buffer containing 100 mM Hepes, 10% sucrose, 0.1% NP-40, and 10 mM dithiothreitol (pH = 7.5) on ice. The homogenates were taken through three freeze/thaw cycles and were subsequently centrifuged at 1,5000×g for 30 min at 4 °C. The supernatant was then combined with 0.3 mL of protease assay buffer containing 10% sucrose, 0.1% CHAPS, 100 mM Hepes, pH 7.5, and 5 μL corresponding fluorometric substrates of caspase-3 and caspase-9, Ac-DEVD-AMC (Biomol) and Ac-LEHD-AMC (Biomol), respectively. After this, the mixture was incubated for 1 h at 37 °C. Finally, fluorescence intensity was read using a spectrophotometer (excitation 360 nm/emission 460 nm).

2.11. Warner-Bratzler shear force (WBSF) determination

The WBSF was determined using the method of Khan et al. (2014). Steaks were packed into cooking bags and immersed in a thermostatic water bath (Jinghong Technology Ltd., Shanghai, China) kept at 80 °C until the temperature at the geometric center of the product reached 75 °C. Afterward, the steaks were removed from the water bath and subjected to cool down at 3 ± 1 °C overnight. Prior to testing, the steaks were then allowed to equilibrate to room temperature (AMSA, 1995). Then, six muscle cylinder cores (Φ = 1.27) were excised along the muscle fiber direction. The muscle cores were sheared perpendicular to the longitudinal orientation with a muscle tenderness meter (C-LM4, Harbin, China), and the WBSF was assayed as the average of the maximal force (Newton (N)) for all six cores for each steak.

2.12. Hematoxylin-eosin (HE) staining

HE staining was performed in accordance with Chen et al. (2020). After each storage period, tissue specimens were fixed with 10% neutral-buffered formalin, and embedded in paraffin wax. Subsequently, sections of 5 μm thickness were stained with hematoxylin-eosin staining and observed under an Olympus IX71 light microscope (Olympus Optical Co. Ltd., Tokyo, Japan).

2.13. Scanning electron micrograph (SEM)

The SEM assay was performed referring to Qian et al. (2020). Briefly, muscle samples were cut into a uniform size (0.3 mm × 0.3 mm × 0.5 mm) and fixed with 3% glutaraldehyde at 4 °C overnight. Following three rinses with 0.1 M phosphoric acid buffer (pH 7.4), the samples were postfixated with 1% osmic acid for another 2 h and dehydrated using varying concentrations of alcohol. After dehydration, the myofibrils were fixed in isoamyl acetate, critical-point dried, sputter coated in gold, and analyzed with a scanning electron microscope (JSM 5600, JOEL Co., Tokyo, Japan).

2.14. Data analysis

The data were analyzed and represented as means ± standard deviations (SD) using SPSS statistical software package (IBM, Chicago, IL,

USA). The means of differences were determined with LSD and Duncan's multiple range tests ($P < 0.05$).

3. Results

3.1. Catechin alleviates oxidative stress in postmortem bovine LTL muscle

Oxidative stress occurs when there is an unbalance between endogenous antioxidant defense and ROS production. The administration of catechin had a significant impact on the oxidant/antioxidant status, as evidenced by the reduction in ROS levels observed during 24–120 h (Fig. 1A). Under normal physiological conditions, a sophisticated antioxidant defense system, comprising enzymes, such as SOD and GSH-Px, is established to counteract oxidative stress. SOD activities during 24–120 h, as well as GSH-Px activities during 24–72 h, were observed to be significantly increased in the presence of catechin compared to its absence ($P < 0.05$; Fig. 1B,C). GPX4, as a constituent of the glutathione peroxidases, functions to reduce lipid hydroperoxides in cell membranes to lipid alcohols by utilizing GSH as an electron donor, thereby inhibiting lipid peroxidation (Liu et al. 2023). The induced GPX4 protein in the steaks following catechin treatment at 24 and 120 h postmortem ($P < 0.05$; Fig. 1D) suggests that the function of GPX4 was enhanced. MDA is a decomposition product of peroxidized polyunsaturated fatty acids, therefore, it is frequently used as a biomarker of oxidative stress. The changes noted in MDA levels were in accordance with the trend detected for the ROS production among the treatments (Fig. 1E). Catechin-injected steaks had consistently lower MDA contents throughout aging ($P < 0.05$) than their control counterparts. In totality, these results established the potential of catechin as an effective antioxidant to mitigate oxidative stress and served as a natural preservative in bovine meat.

3.2. Catechin suppresses autophagy in postmortem bovine LTL muscle

The cytosolic ratio of LC3 has been widely adopted as a novel index for autophagy induction (Karim et al., 2007). To clarify the forms of LC3, the conversions of which were assayed by immunoblotting using an antibody recognizing both distinct forms of LC3, namely, LC3-I and LC3-II. In this study, catechin was found to impede the conversion of LC3-I to LC3-II, with the highest expressions of LC3-II at 120 h ($P < 0.05$; Fig. 2A, B). Coherent with the reduced LC3-II/LC3-I ratio, other essential autophagy-modulating proteins were also affected by catechin. The intensity of the Atg7 band, crucial for autophagosome biogenesis, was considerably lower following catechin treatment compared to the control throughout aging ($P < 0.05$; Fig. 2A, C). Accordingly, an inhibitory effect by the catechin was also found toward Beclin-1 expression, a core protein in autophagy machinery during 24–120 h postmortem ($P < 0.05$; Fig. 2A, D). Overall, the above-mentioned data corroborated the role of catechin in autophagy inhibition.

3.3. PI3K/Akt/mTOR pathway engages catechin-suppressed autophagy in postmortem bovine LTL muscle

PI3K/Akt/mTOR signaling pathway is arguably the most significant mediator in skeletal muscle given its involvement in various biological consequences related to both survival and death (Ni et al., 2012). To further explore initial underlying molecular mechanisms of catechin-mediated autophagy inhibition. The levels of PI3K, Akt, and mTOR, as well as their phosphorylation levels, were investigated by western blot (Fig. 3). Substantial upregulation of the p-PI3K/PI3K ratio was detected in catechin-treated steaks than the controls throughout aging ($P < 0.05$; Fig. 3A, B). Similarly, Akt, a major downstream effector of PI3K, was significantly magnified by catechin during 72–120 h ($P < 0.05$; Fig. 3A, C). Subsequently, PI3K/Akt pathway activation is annotated with negative regulation autophagy by targeting the downstream mTOR complex. The p-mTOR/mTOR ratios were almost two times that of the

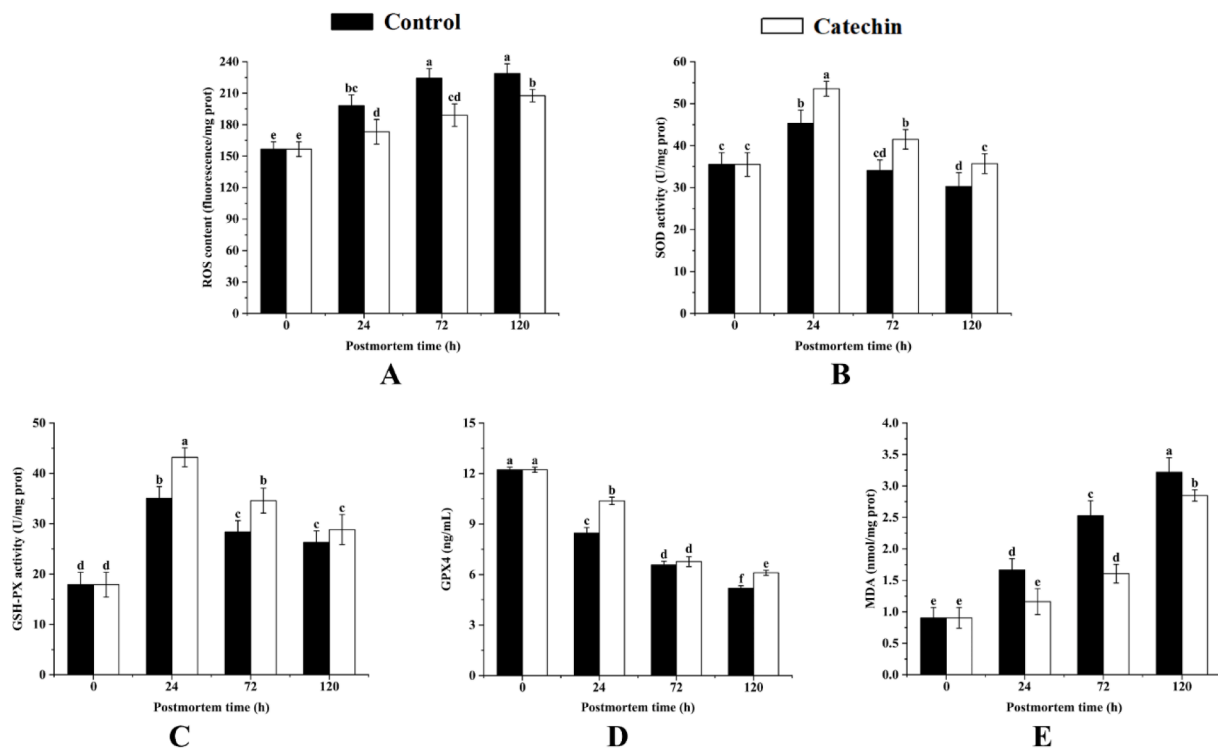


Fig. 1. ROS production (A), SOD activity (B), GSH-Px activity (C), GPX4 levels (D), and MDA level (E) of postmortem bovine LTL muscle treated with 0.9% saline and 300 μM green tea catechin aged at 4 °C for 0, 24, 72, and 120 h. Bars labeled with different letters are significantly different from each other at $P < 0.05$.

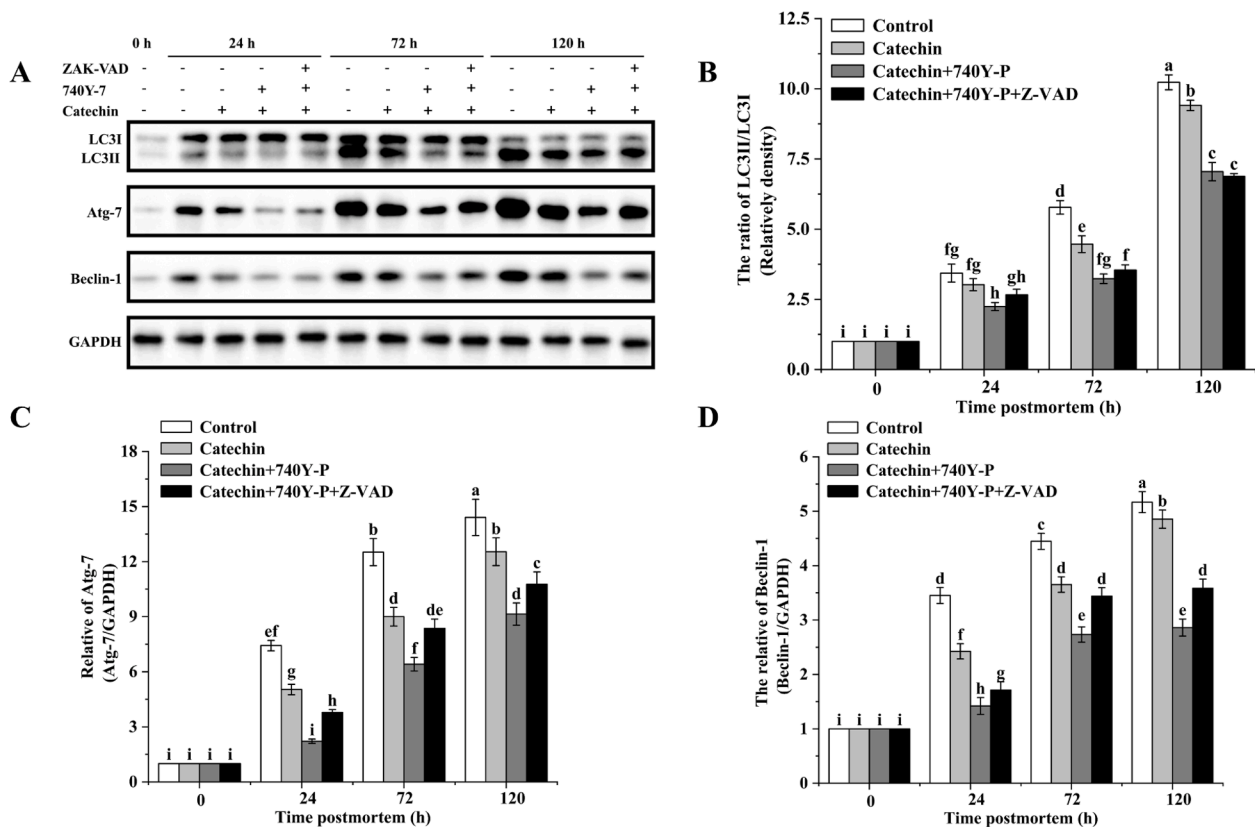


Fig. 2. Representative western blot of LC3-I, LC3-II, Atg7, and Beclin-1 (A). Densitometric analysis of LC3-II/LC3-I ratio (B), Atg7 (C), and Beclin-1 (D) of post-mortem bovine LTL muscle treated with 0.9% saline, 300 μM green tea catechin, 300 μM green tea catechin + 150 μM 740Y-P aged at 4 °C for 0, 24, 72, and 120 h. The ratio was calculated as the band intensity from a given time over the postmortem 0 h. Bars labeled with different letters are significantly different from each other at $P < 0.05$.

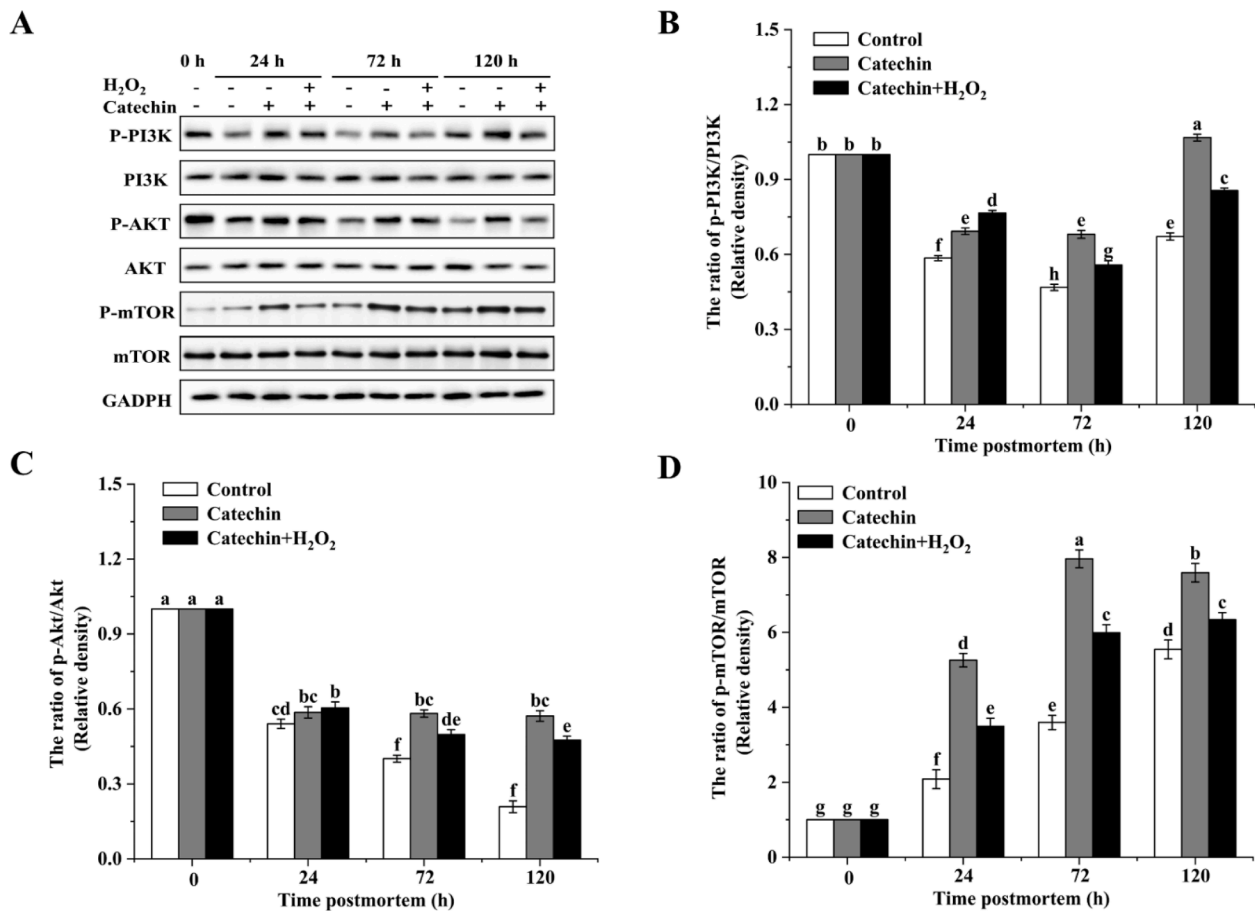


Fig. 3. Representative western blot of p-PI3K, PI3K, p-Akt, Akt, and p-mTOR, and mTOR (A). Densitometric analysis of p-PI3K/PI3K (B), p-Akt/Akt (C), and p-mTOR/mTOR (D) of postmortem bovine LTL muscle treated with 0.9% saline, 300 μ M green tea catechin, 300 μ M green tea catechin + 150 μ M 740Y-P aged at 4 $^{\circ}$ C for 0, 24, 72, and 120 h. The ratio was calculated as the band intensity from a given time over the postmortem 0 h. Bars labeled with different letters are significantly different from each other at $P < 0.05$.

control at 24 and 72 h ($P < 0.05$; Fig. 3A, D). Unexpectedly, 740Y-P (a PI3K/Akt/mTOR signaling linkage activator) caused a greater extent decrease in the LC3-II/LC3-I ratio, Atg7, and Beclin-1 expression throughout the aging process than the catechin-treated group ($P < 0.05$; Fig. 2), suggesting that 740Y-P further enhances the inhibitory efficacy of catechin on autophagy. Overall, the above results seemed to confirm our hypothesis that catechin inhibited autophagy, at least in part, via triggering PI3K/Akt/mTOR kinase activity.

3.4. Attenuated oxidative stress is involved with catechin-inhibited autophagy in postmortem bovine LTL muscle

It is well appreciated that oxidative stress is related to autophagy activation in postmortem muscle. Our findings demonstrate that catechin effectively alleviated oxidative stress (Fig. 1). Remarkably, these effects coincide with reduced autophagic responses while negatively correlated with the activated PI3K/Akt/mTOR pathway (Figs. 2-3). This made us assume that catechin may play a pivotal role in preventing the degree of oxidative stress, which could serve as a crucial factor in inducing the PI3K/Akt/mTOR pathway, thereby modulating autophagy. As seen in Fig. 3A, catechin-induced activation of p-PI3K/PI3K and p-Akt/Akt ratios during 72–120 h, as well as p-mTOR/mTOR ratio throughout aging, were significantly reversed by the introduction of an oxidative stress inducer, H₂O₂ ($P < 0.05$; Fig. 3). The above results illustrate that catechin may inhibit autophagy in a PI3K/Akt/mTOR pathway-dependent manner by alleviating oxidative stress.

3.5. Catechin suppresses the mitochondrial intrinsic pathway of apoptosis via alleviating oxidative stress in postmortem bovine LTL muscle

Mitochondria are identified as central regulators of apoptosis. The MPTP opening dynamics at various stages were then examined. Post-mortem oxidative stress was found to evoke irreversible MPTP opening levels (Fig. 4A). However, the observed change was substantially prevented by catechin administration during 24–72 h ($P < 0.05$). Correspondingly, MMP was assessed by red/green fluorescence intensity, which relies only on the membrane potential but is independent of other factors. Following catechin administration, a reduction in fluorescence emission from red to green was observed during 24–120 h ($P < 0.05$; Fig. 4B). The above data is indicative of decreases in MPTP opening and collapse of MMP, subsequently the inhibition of normal mitochondrial dysfunction was caused by catechin.

The expression levels of Bcl-2 family members were determined in recognition of their role in the mitochondrial apoptotic pathway (Lindqvist et al., 2014). The Bax/Bcl-2 ratio enhanced gradually in a time-dependent manner ($P < 0.05$; Fig. 4C-F), consistent with previous studies on Bcl-2 family protein levels in postmortem muscle (Wang et al., 2018a). However, the Bax/Bcl-2 ratios in catechin-injected steaks consistently showed significantly lower values throughout aging versus controls ($P < 0.05$), suggesting that attenuated oxidative stress caused by catechin concomitantly downregulated the Bax/Bcl-2 ratio. TUNEL assay is a classic technique widely applied to determine apoptotic nuclei in muscle tissues and cells. The representative images of TUNEL-stained cells were presented in Fig. 4G and the quantification of apoptotic

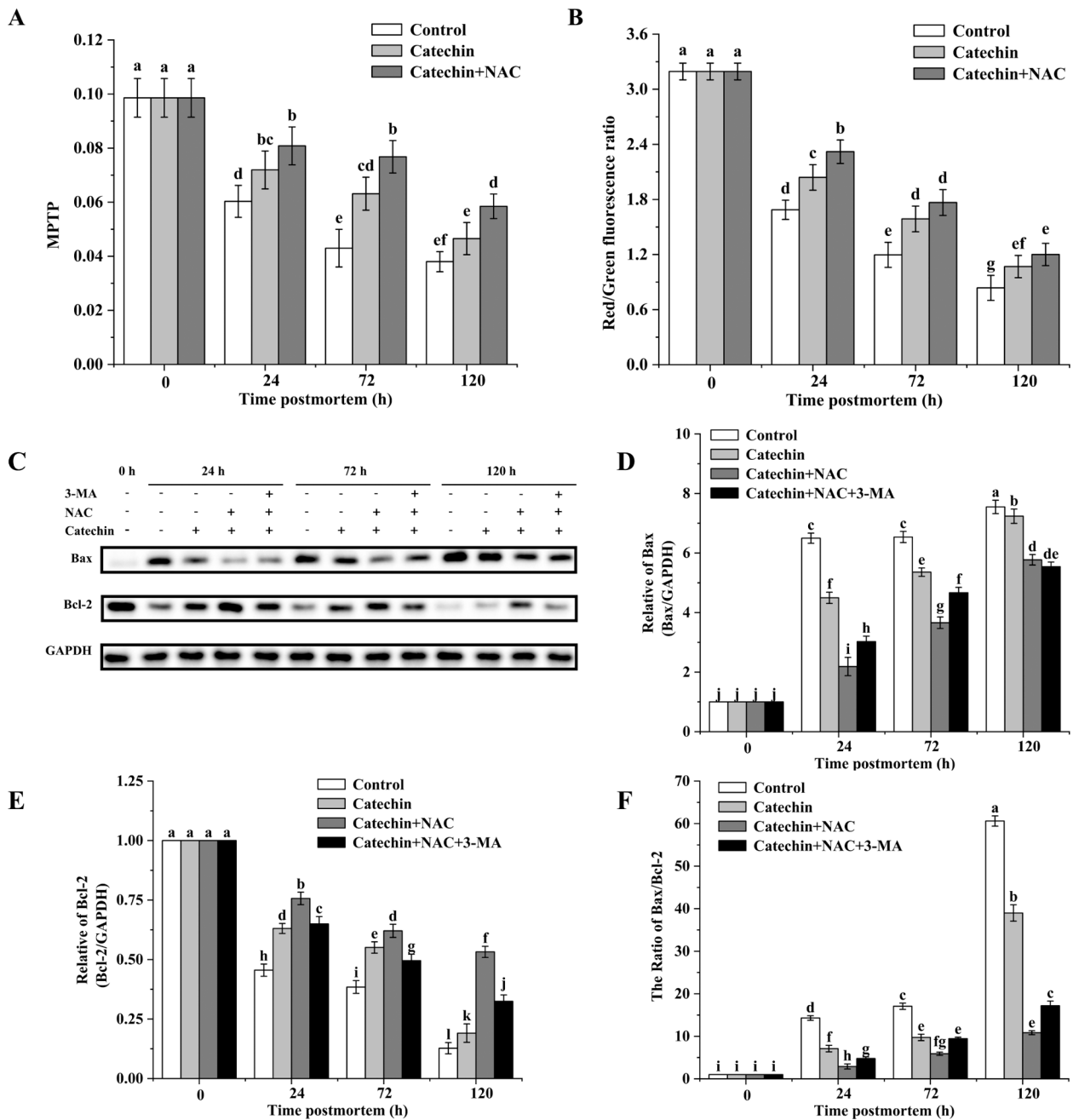


Fig. 4. Mitochondrial membrane permeability transition opening (A), mitochondrial membrane potential (B), representative western blot of Bax and Bcl-2 (C), densitometric analysis of Bax (D), Bcl-2 (E), Bax/Bcl-2 ratio (F), TUNEL photographs of the apoptotic nucleus (G), negative and positive controls for the TUNEL assay (H), TUNEL positive nucleus counts (I), activities of caspase-9 (J) and caspase-3 (K) of postmortem bovine LTL muscle treated with 0.9% saline, 300 μM green tea catechin, 300 μM green tea catechin + 20 mM NAC, 20 mM green tea catechin + 20 mM NAC + 10 mM 3-MA aged at 4 °C for 0, 24, 72, and 120 h. Bars labeled with different letters are significantly different from each other at $P < 0.05$. (For interpretation of the references to color in this figure legend, the reader is referred to the web version of this article.)

nucleus counts was illustrated in Fig. 4I. None of the negative controls showed any TUNEL-positive signals, whereas TUNEL staining was observed in all positive controls (Fig. 4H). Studies with the muscle at 0 h showed a faint/barely perceptible TUNEL signal, which progressively became stronger and randomly distributed over aging. Importantly, the administration of catechin resulted in a notable reduction in the number of apoptotic nuclei in comparison to the control group during 24–120 h ($P < 0.05$). To ascertain the influences of catechin on the apoptotic cascade reaction, both caspase-9 and caspase-3 activities were evaluated. As depicted in Fig. 4J and K, catechin exhibited a significant suppression of caspase-9 activities during 24–72 h and caspase-3

activities during 72–120 h ($P < 0.05$), demonstrating the inhibition of caspase-dependent apoptosis.

Subsequently, whether the catechin-prevented mitochondrial apoptotic pathway is concerned with attenuated oxidative stress was examined. Specifically, ROS scavenger (*N*-Acetyl-l-cysteine, NAC) significantly further exacerbated the inhibitory effect of catechin on MPTP opening and MMP collapse ($P < 0.05$; Fig. 4A–B), illustrating that catechin may impair mitochondrial dysfunction by diminishing oxidative stress. As a result, NAC markedly further decreased Bax/Bcl-2 ratio, thereby relieving apoptotic injury and the activation of caspase-3 and caspase-9 cascades when compared to the catechin group (Fig. 4C–K).

Based on these observations, we tentatively concluded that oxidative stress may play a major role in catechin-induced inhibition of the mitochondrial apoptotic pathways.

3.6. Autophagy and apoptosis can cross-inhibit each other under catechin regulation in postmortem bovine LTL muscle

Apoptosis and autophagy share common regulatory properties and the relationship between them is not fully understood. Thus, we next explored whether autophagy serves as the mechanistic link underlying the catechin-induced reduction of apoptosis. Particularly, 3-MA (a specific autophagy inhibitor) partly reversed the inhibition of apoptotic nucleus counts and apoptotic markers, including Bax/Bcl-2 ratios, caspase-9, and caspase-3 activities (Fig. 4C-K) induced by H₂O₂ and catechin. In turn, Z-VAD (a specific apoptosis inhibitor) tended to block the autophagy suppression induced by catechin and 740Y-P, as evidenced by the autophagic biomarkers LC3-II/LC3-I ratio, Beclin-1, and Atg-7 levels (Fig. 2). Although unexpected, this response supports previous reports indicating that caspase inhibitors facilitate autophagy (Xi et al., 2011). Overall, the data suggest that both autophagy and apoptosis were inhibited under catechin regulation, with the two processes mutually inhibiting one another.

3.7. Catechin hampers the tenderization pattern in postmortem bovine LTL muscle

WBSF is a reliable and intuitive indicator inversely reflecting meat tenderness. An evident difference occurred in tenderization rate between the two groups (Fig. 5A). The WBSF values peaked at 24 h in both groups, coinciding with the onset of rigor mortis, with values of 75.14 and 84.52 N in the control and catechin treatments, respectively. Following, a more rapid decline in WBSF was observed in the absence of catechin than in the presence during 24–72 h. The abovementioned results support the action of catechin in meat tenderization inhibition. This level was considered for microstructural studies and the observations of muscles were visualized by SEM. The results depicted in Fig. 5B demonstrate that myofibrillar structures were contiguously and more neatly arranged in the postmortem 0 h. However, mild separation of individual myofibers occurred in the samples subjected to 24 h. At 72 h, the muscle fiber architectures were disrupted, and at 120 h, large areas of breakage and dissolution of myofibrillar structures appeared. Instead, catechin led to less disintegration, and the gaps among myofibrils were attenuated to some extent, especially at 24 and 72 h. Subsequently, the muscle fiber diameter and muscle cell gap were observed by H&E staining, and representative staining was presented in Fig. 5C. Cells at 0 h were structural integrity and well-distributed nucleoplasm, with narrow gaps between muscle fiber bundles and scarcely any injuries. Over aging, myofiber was organized into flake architectures, the distance between myofibers increased, and cavitation phenomena appeared in the muscle bundles. These properties align with the results of Hou et al. (2020) that muscle fibers shrunk obviously during postmortem aging. However, myofibrils from the catechin group exhibited larger diameters, reduced intermyofibrillar spacing, and alleviated degrees of myofibril fragmentation in comparison to the control during 24–120 h. These changes were in line with the WBSF and SEM findings. Totally, although acts as a preservative, catechin may hamper the meat tenderization pattern of postmortem bovine muscle.

4. Discussion

Green tea catechin is a naturally occurring plant flavonoid that has been shown to be a therapeutic agent of its antioxidative properties (Namal Senanayake, 2013). Sudden cessation of blood flow results in an anoxia situation in postmortem muscle, and this tissue hypoxia causes mitochondrial dysfunction, contributing to disturbed redox homeostasis and enhanced ROS production to initiate oxidative stress (Lana & Zolla,

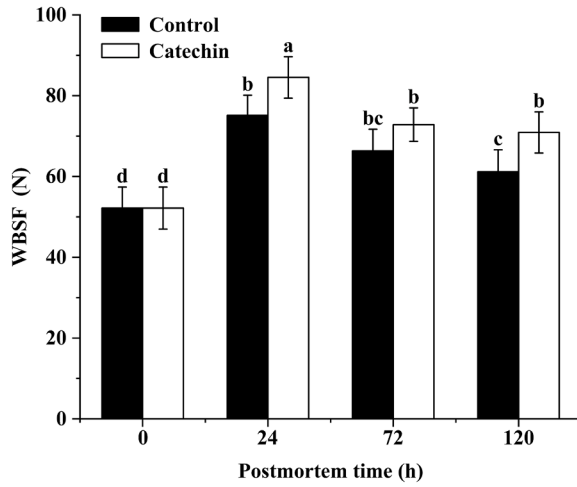
2015). Eventually, the damage to biological macromolecules induced by the stress leads to cell death like apoptosis and autophagy (García-Macia et al., 2014). Thus, oxidative stress is recognized as a major cause influencing protein functionality and sensory, nutritional, and shelf-life qualities of meat. In this study, catechin-injected steaks engaged a generalized suppressed oxidative stress, as evidenced by reduced ROS and oxidized product generation, whereas increased activities of anti-oxidant enzymes. Similar findings have been reported that dietary natural supplementation with natural antioxidants, such as EGCG (Zhao et al., 2021) and curcumin (Zhang et al., 2018, Zhang et al., 2018) are effective strategies to combat redox imbalance in broilers. Additionally, linalool, limonene, and sabinene reduce oxidative damage of MDA to the myofibrillar protein of rabbit meat (Wang et al., 2021).

The muscle-to-meat transformation period appeared to conform to the hallmarks of autophagy and apoptosis since oxidative stress is central in both mechanisms. It remains unclear, however, whether catechin affects apoptosis and autophagy in postmortem muscle. Autophagy is a self-degradation process that regulates the balance between cell death and survival (García-Macia et al., 2014). Postmortem aging is a highly nutrient and energy-deprivation process. Therefore, autophagy has been proposed to play a developmental role in meat tenderization (García-Macia et al., 2014). The present study demonstrates that catechin inhibits autophagic features including the LC3-II/LC3-I ratio, and the expressions of Beclin-1 and Atg-7. This finding supports the emerging understanding of the role of autophagy in the postmortem aging of different beef breeds (García-Macia et al., 2014). Furthermore, several studies have depicted the inhibitory effect of catechin on autophagy in microglial cells (Chen et al., 2016). Analogously, EGCG, the major catechin in green tea extract, exerts a protective role in autophagy in the ischemic myocardium (Zhang et al., 2019).

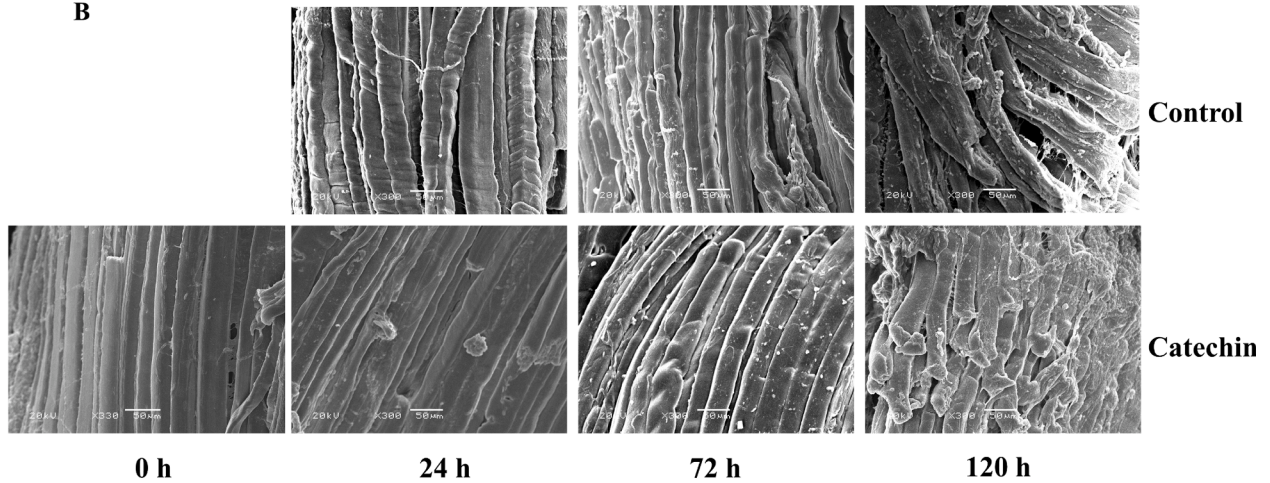
To further study the underlying mechanism by which catechin suppresses autophagy, potential downstream pathways were examined. Specifically, we focused on the PI3K/Akt/mTOR pathway, a vital cell survival cascade that typically suppresses autophagy. The inhibitory state of autophagy caused by catechin was magnified by PI3K/Akt/mTOR activator 740Y-P. Unsurprisingly, the classic oxidative stress inducer H₂O₂ blocked catechin-induced PI3K/Akt/mTOR activation, implying that oxidative stress places upstream of PI3K/Akt/mTOR pathway activation and autophagy inhibition. The relationship between ROS and autophagy is complex. In most cases, autophagy is triggered by oxidative stress through the regulation of PI3K/Akt/mTOR signaling activation (Koundouros & Poulogiannis, 2018). Our findings corroborate previous research indicating that PI3K/Akt/mTOR is indirectly engaged in ROS-mediated microglia autophagy upon catechin treatment (Chen et al., 2016). However, in 3 T3-L1 preadipocytes, EGCG down-regulates the PI3K/Akt/mTOR pathway along with ROS suppression and cell death induction (Kumar et al., 2019), which seems contrary to our results, possibly due to different contexts of oxidative stress and animal models.

Compared with autophagy occurring within hours of animal killing, apoptosis is an extensively studied cell death modality and a critical early step in the tenderization process (Zhang et al., 2018, Zhang et al., 2018). In this study, catechin declined apoptotic nucleus counts. Generally, apoptosis is modulated by a myriad of factors, of which mitochondria homeostasis, a target of oxidative stress, is the most prevalent one. As expected, catechin protected against mitochondrial dysfunction, and its effect was further strengthened through a combination of NAC. The same effect was observed in human lung fibroblasts that catechin ameliorates oxidative stress and mitochondrial dysfunction (Silva Santos et al., 2017). Besides, catechin mitigated the Bax/Bcl-2 ratio, which is a cell apoptosis switch that exquisitely modulates the formational state of MPTP. This was found to be in parallel with catechin-induced impairment of mitochondrial dysfunction. Consequently, catechin inhibited mitochondrial apoptosis cascade reaction, thereby inhibiting caspase-9/3 activities in response to a blunted oxidative stress. These findings corroborate previous reports that

A



B



C

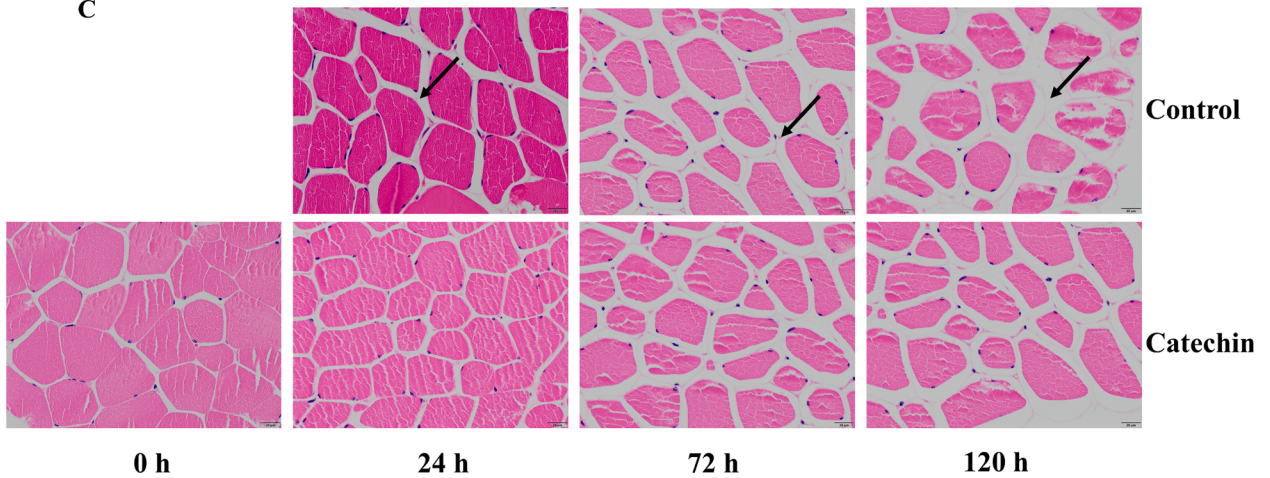


Fig. 5. Warner-Bratzler shear force (A), scanning electron microscopy, scale bar = 50 μm (B), and hematoxylin and eosin staining of muscle fiber bundles, scale bar = 20 μm (C) of postmortem bovine LTL muscle treated with 0.9% saline and 300 μM green tea catechin aged at 4 $^{\circ}\text{C}$ for 0, 24, 72, and 120 h. Bars labeled with different letters are significantly different from each other at $P < 0.05$. (For interpretation of the references to color in this figure legend, the reader is referred to the web version of this article.)

catechin inactivates caspases to attenuate apoptosis by scavenging ROS (Chen et al., 2016). Similarly, *EPI*, a member of the catechin family, effectively reduces mitochondrial apoptosis in neonatal mouse cardiomyocytes (Li et al., 2018).

Apoptotic and autophagic death interplay antagonistically, additively, or even synergistically relying on muscle type, environment, and stimulus resources (Lana & Zolla, 2015). In certain contexts, a tiny prevalence of either mechanism may tip the balance one way or the other. The results of our study demonstrate that catechin inhibits both autophagy and apoptosis simultaneously. Interestingly, these two mechanisms of death reciprocally inhibit each other (Figs. 2, 4), fitting well into the known concepts of the crosstalk between autophagy and apoptosis (Lana & Zolla, 2015). Considerable evidence has implicated that the pathways involved in apoptosis and autophagy can be crosstalk including Atg and Bcl family proteins (Mukhopadhyay et al., 2014). Indeed, certain apoptotic proteins, apparently like Bcl-2 and Bcl-xl, or Mcl-1 function in Beclin-1-mediated autophagy (Pyo et al., 2012). From this perspective, Bim has been identified to decrease autophagy independently of its pro-apoptotic function (Lindqvist et al., 2014). Nevertheless, the present study is the primary step for the novel considerations for apoptosis and autophagy crosstalk, and the specific mode of action following catechin administration. Further research is warranted to expand upon these findings.

Ultimately, catechin suppressed myofibril degradation and impeded the tenderization process of postmortem bovine muscle. Oxidative stress has been proven to contribute to proteolytic susceptibility of myofibrillar and consequent tenderization of muscle (Malheiros et al., 2019). This notion is further confirmed by the findings that NAC inhibits tenderness of bovine muscle (Chen et al., 2020). Additionally, pasture feeding enhances the antioxidant capacity while reducing lamb tenderness (Luo et al., 2019). Nevertheless, herbal extracts possessing potent antioxidant properties improve the tenderness of muscle *longissimus lumborum* while failing to achieve statistical significance in *semimembranosus* (Modzelewska-Kapituła et al., 2018). The above differences may be attributed to muscle types, species differences, or distinct targeting mechanisms functioning. The significance of considering apoptosis to understand tenderization either directly or indirectly *in vitro* and *in vivo* has been attested. In this process, the intervention of apoptotic behavior, reflected in apoptotic effectors like caspases, has been highlighted to beef aging and tenderization (Hou et al., 2020; Huang et al., 2009). These are compatible with our result that catechin partially inactivated caspase-9/3, which may offer a potential explanation for the observed reduction in tenderness following catechin treatment. Additionally, regarding the short period after slaughter, the autophagic behavior of slaughtered muscle could also provide partial answers to meat tenderness. Particularly, bovine muscle undergoes autophagy shortly after slaughter (24 h) to counteract the abrupt hypoxia, facilitating the preliminary phases of meat tenderization (García-Macia et al., 2014), and autophagy was facilitated by quercetin to enhance tenderness in chickens (Wang et al., 2022). Of greater significance is the hypothesis that the proportion of apoptotic and autophagic cells within distinct muscle cells employing diverse strategies may serve as a pivotal factor in the postmortem tenderization process, (Lana & Zolla, 2015), although not specifically investigated in this study.

5. Conclusion

In conclusion, this study provides evidence that catechin can alleviate oxidative stress in postmortem bovine LTL muscle while hindering the tenderization pattern. This effect is mediated by the inhibition of autophagy through the activation of the oxidative stress-sensitive PI3K/Akt/mTOR signaling pathway, and concurrent suppression of the mitochondrial apoptosis pathway. Moreover, autophagic and apoptotic death cross-inhibit each other. These features may offer novel ideas of autophagy and apoptosis in improving bovine muscle tenderization and reveal the notion that catechin acts as a preservative and antioxidant in

meat preservation during storage, nevertheless, in the meantime, exert adverse influences on bovine aging and tenderness.

CRedit authorship contribution statement

Xijin Zhu: Investigation, Writing – original draft, Formal analysis. **Aixia Li:** Software, Formal analysis, Writing – review & editing. **Nan Sun:** Investigation, Visualization. **Ling Han:** Project administration, Funding acquisition. **Qunli Yu:** Methodology, Conceptualization.

Declaration of Competing Interest

The authors declare that they have no known competing financial interests or personal relationships that could have appeared to influence the work reported in this paper.

Data availability

No data was used for the research described in the article.

Acknowledgments

The authors are very grateful for the financial support from “the National Natural Science Foundation of China (No.32060553)”, and “the National Key research and Development (No. 2021YFD1600204-2)”. The authors are indebted to the editor and reviewers for their valuable comments and suggestions that helped to improve the manuscript.

Informed Consent

Informed consent was obtained from all individual participants included in the study.

References

- AMSA. (1995). *Research guidelines:cooking, sensory evaluation, and instrumental tenderness measurements of fresh meat*. Centennial, CO: American Meat Science Association in cooperation with the National Livestock and Meat Board (now the Cattlemen's Beef Association).
- Breneselová, M., Koréneková, B., Ma, J., Marcin, S., Jevinová, P., Pipová, M., & Turek, P. (2015). *Effects of vacuum packaging conditions on the quality, biochemical changes and the durability of ostrich meat*. 101, 42–47. <https://doi.org/10.1016/j.meatsci.2014.11.003>.
- Bu, L., Zheng, T., Mao, C., Wu, F., Mou, X., Xu, C., ... Wang, X. (2021). Autophagy inhibition contributes to epigallocatechin-3-gallate-mediated apoptosis in papillary thyroid cancer cells. *Molecular and Cellular Toxicology*, 17(4), 533–542. <https://doi.org/10.1007/s13273-021-00164-3>
- Cao, J. X., Ou, C. R., Zou, Y. F., Ye, K. P., Zhang, Q. Q., Khan, M. A., ... Zhou, G. (2013). Activation of caspase-3 and its correlation with shear force in bovine skeletal muscles during postmortem conditioning. *Journal of Animal Science*, 91(9), 4547–4552. <https://doi.org/10.2527/jas.2013-6469>
- Chen, C. M., Wu, C. T., Yang, T. H., Chang, Y. A., Sheu, M. L., & Liu, S. H. (2016). Green tea catechin prevents hypoxia/reperfusion-evoked oxidative stress-regulated autophagy-activated apoptosis and cell death in microglial cells. *Journal of Agricultural and Food Chemistry*, 64(20), 4078–4085. <https://doi.org/10.1021/acs.jafc.6b01513>
- Chen, C., Zhang, J., Guo, Z., Shi, X., Zhang, Y., Zhang, L., ... Han, L. (2020). Effect of oxidative stress on AIF-mediated apoptosis and bovine muscle tenderness during postmortem aging. *Journal of Food Science*, 85(1), 77–85. <https://doi.org/10.1111/1750-3841.14969>
- Chen, T., Zhou, G. H., Xu, X. L., Zhao, G. M., Li, C., & bao. (2010). Phospholipase A2 and antioxidant enzyme activities in normal and PSE pork. *Meat Science*, 84(1), 143–146. <https://doi.org/10.1016/j.meatsci.2009.08.039>
- Du, B., Lin, P., & Lin, J. (2022). ECGG and ECG induce apoptosis and decrease autophagy via the AMPK/mTOR and PI3K/AKT/mTOR pathway in human melanoma cells. *Chinese Journal of Natural Medicines*, 20(4), 290–300. [https://doi.org/10.1016/S1875-5364\(22\)60166-3](https://doi.org/10.1016/S1875-5364(22)60166-3)
- Du, X., Mawolo, J. B., Liu, X., Mi, X., Li, Q., & Wen, Y. (2021). Expression and distribution of neuroglobin and hypoxia-inducible factor-1 α in the adult yak telencephalon. *Veterinary Medicine and Science*, 7(5), 1707–1717. <https://doi.org/10.1002/vms3.553>
- García-Macia, M., Sierra, V., Palanca, A., Vega-Naredo, I., De Gonzalo-Calvo, D., Rodríguez-González, S., ... Coto-Montes, A. (2014). Autophagy during beef aging. *Autophagy*, 10(1), 137–143. <https://doi.org/10.4161/auto.26659>

- Herrera-Mendez, C. H., Becila, S., Boudjellal, A., & Ouali, A. (2006). Meat ageing: Reconsideration of the current concept. *Trends in Food Science and Technology*, 17(8), 394–405. <https://doi.org/10.1016/j.tifs.2006.01.011>
- Hou, Q., Liu, R., Tian, X., & Zhang, W. (2020). Involvement of protein S-nitrosylation in regulating beef apoptosis during postmortem aging. *Food Chemistry*, 326, Article 126975. <https://doi.org/10.1016/j.foodchem.2020.126975>
- Huang, M., Huang, F., Xu, X., & Zhou, G. (2009). Influence of caspase3 selective inhibitor on proteolysis of chicken skeletal muscle proteins during post mortem aging. *Food Chemistry*, 115(1), 181–186. <https://doi.org/10.1016/j.foodchem.2008.11.095>
- Karim, M. R., Kanazawa, T., Daigaku, Y., Fujimura, S., Miotto, G., & Kadowaki, M. (2007). Cytosolic LC3 ratio as a sensitive index of macroautophagy in isolated rat hepatocytes and H4-II-E cells. *Autophagy*, 3(6), 553–560. <https://doi.org/10.4161/aut.4615>
- Khan, M. A., Ali, S., Abid, M., Cao, J., Jabbar, S., Tume, R. K., & Zhou, G. (2014). Improved duck meat quality by application of high pressure and heat: A study of water mobility and compartmentalization, protein denaturation and textural properties. *Food Research International*, 62, 926–933. <https://doi.org/10.1016/j.foodres.2014.04.006>
- Koundouros, N., & Poullogiannis, G. (2018). Phosphoinositide 3-Kinase/Akt signaling and redox metabolism in cancer. *Frontiers in Oncology*, 8(MAY), 2–10. <https://doi.org/10.3389/fonc.2018.00160>
- Kumar, R., Sharma, A., Kumari, A., Gulati, A., Padwad, Y., & Sharma, R. (2019). Epigallocatechin gallate suppresses premature senescence of preadipocytes by inhibition of PI3K/Akt/mTOR pathway and induces senescent cell death by regulation of Bax/Bcl-2 pathway. *Biogerontology*, 20(2), 171–189. <https://doi.org/10.1007/s10522-018-9785-1>
- Lana, A., & Zolla, L. (2015). Apoptosis or autophagy, that is the question: Two ways for muscle sacrifice towards meat. *Trends in Food Science and Technology*, 46(2), 231–241. <https://doi.org/10.1016/j.tifs.2015.10.001>
- Li, J. W., Wang, X. Y., Zhang, X., Gao, L., Wang, L. F., & Yin, X. H. (2018). (-)-Epicatechin protects against myocardial ischemia-induced cardiac injury via activation of the PTEN/PI3K/AKT pathway. *Molecular Medicine Reports*, 17(6), 8300–8308. <https://doi.org/10.3892/mmr.2018.8870>
- Li, J. X., Tong, C. W. C., Xu, D. Q., & Chan, K. M. (1999). Changes in membrane fluidity and lipid peroxidation of skeletal muscle mitochondria after exhausting exercise in rats. *European Journal of Applied Physiology and Occupational Physiology*, 80(2), 113–117. <https://doi.org/10.1007/s004210050566>
- Lindqvist, L. M., Heinlein, M., Huang, D. C. S., & Vaux, D. L. (2014). Prosurvival Bcl-2 family members affect autophagy only indirectly, by inhibiting Bax and Bak. *Proceedings of the National Academy of Sciences of the United States of America*, 111(23), 8512–8517. <https://doi.org/10.1073/pnas.1406425111>
- Liu, J., Hu, Z., Ma, Q., Wang, S., & Liu, D. (2023). Ferritin-dependent cellular autophagy pathway promotes ferroptosis in beef during cold storage. *Food Chemistry*, 412 (January), Article 135550. <https://doi.org/10.1016/j.foodchem.2023.135550>
- Luo, Y., Wang, B., Liu, C., Su, R., Hou, Y., Yao, D., ... Jin, Y. (2019). Meat quality, fatty acids, volatile compounds, and antioxidant properties of lambs fed pasture versus mixed diet. *Food Science and Nutrition*, 7(9), 2796–2805. <https://doi.org/10.1002/fsn3.1039>
- Malheiros, J. M., Braga, C. P., Grove, R. A., Ribeiro, F. A., Calkins, C. R., Adamec, J., & Chardulo, L. A. L. (2019). Influence of oxidative damage to proteins on meat tenderness using a proteomics approach. *Meat Science*, 148, 64–71. <https://doi.org/10.1016/j.meatsci.2018.08.016>
- Modzelewska-Kapitula, M., Tkacz, K., Nogalski, Z., Karpińska-Tymoszczyk, M., Draszanowska, A., Pietrzak-Fiecko, R., ... Lipiński, K. (2018). Addition of herbal extracts to the Holstein-Friesian bulls' diet changes the quality of beef. *Meat Science*, 145, 163–170. <https://doi.org/10.1016/j.meatsci.2018.06.033>
- Mukhopadhyay, S., Panda, P. K., Sinha, N., Das, D. N., & Bhutia, S. K. (2014). Autophagy and apoptosis: Where do they meet? *Apoptosis*, 19(4), 555–566. <https://doi.org/10.1007/s10495-014-0967-2>
- Namal Senanayake, S. P. J. (2013). Green tea extract: Chemistry, antioxidant properties and food applications - A review. *Journal of Functional Foods*, 5(4), 1529–1541. <https://doi.org/10.1016/j.jff.2013.08.011>
- Ni, J., Liu, Q., Xie, S., Carlson, C., Von, T., Vogel, K., ... Zhao, J. (2012). Functional characterization of an isoform-selective inhibitor of PI3K-p110 β as a potential anticancer agent. *Cancer Discovery*, 2(5), 425–433. <https://doi.org/10.1158/2159-8290.CD-12-0003>
- Pyo, J. O., Nah, J., & Jung, Y. K. (2012). Molecules and their functions in autophagy. *Experimental and Molecular Medicine*, 44(2), 73–80. <https://doi.org/10.3858/emmm.2012.44.2.029>
- Qian, S., Li, X., Wang, H., Wei, X., Mehmood, W., Zhang, C., & Blecker, C. (2020). Contribution of calpain to protein degradation, variation in myowater properties and the water-holding capacity of pork during postmortem ageing. *Food Chemistry*, 324, Article 126892. <https://doi.org/10.1016/j.foodchem.2020.126892>
- Silva Santos, L. F., Stolfo, A., Calloni, C., & Salvador, M. (2017). Catechin and epicatechin reduce mitochondrial dysfunction and oxidative stress induced by amiodarone in human lung fibroblasts. *Journal of Arrhythmia*, 33(3), 220–225. <https://doi.org/10.1016/j.joa.2016.09.004>
- Tian, L., & Huang, J. (2019). Antioxidant effects of tea catechins on the shelf life of raw minced duck meat. *Food Science and Technology (Brazil)*, 39(1), 59–65. <https://doi.org/10.1590/fst.25217>
- Wang, L. L., Yu, Q. L., Han, L., Ma, X. L., Song, R. D., Zhao, S. N., & Zhang, W. H. (2018a). Study on the effect of reactive oxygen species-mediated oxidative stress on the activation of mitochondrial apoptosis and the tenderness of yak meat. *Food Chemistry*. <https://doi.org/10.1016/j.foodchem.2017.10.034>
- Wang, L. L., Yu, Q. L., Han, L., Ma, X. L., Song, R. D., Zhao, S. N., & Zhang, W. H. (2018b). Study on the effect of reactive oxygen species-mediated oxidative stress on the activation of mitochondrial apoptosis and the tenderness of yak meat. *Food Chemistry*, 244(September 2017), 394–402. <https://doi.org/10.1016/j.foodchem.2017.10.034>
- Wang, T., Feng, X., Li, L., Luo, J., Liu, X., Zheng, J., ... Chen, L. (2022). Effects of quercetin on tenderness, apoptotic and autophagy signalling in chickens during post-mortem ageing. *Food Chemistry*, 383(February), Article 132409. <https://doi.org/10.1016/j.foodchem.2022.132409>
- Wang, Z., He, Z., Zhang, D., Chen, X., & Li, H. (2021). The effect of linalool, limonene and sabinene on the thermal stability and structure of rabbit meat myofibrillar protein under malondialdehyde-induced oxidative stress. *Lwt*, 148(2), Article 111707. <https://doi.org/10.1016/j.lwt.2021.111707>
- Xi, G., Hu, X., Wu, B., Jiang, H., Young, C. Y. F., Pang, Y., & Yuan, H. (2011). Autophagy inhibition promotes paclitaxel-induced apoptosis in cancer cells. *Cancer Letters*, 307(2), 141–148. <https://doi.org/10.1016/j.canlet.2011.03.026>
- Yan, Y., Chen, X., Huang, J., Huan, C., & Li, C. (2022). H2O2-induced oxidative stress impairs meat quality by inducing apoptosis and autophagy via ROS/NF- κ B signaling pathway in broiler thigh muscle. *Poultry Science*, 101(4), Article 101759. <https://doi.org/10.1016/j.psj.2022.101759>
- Zhang, C., Liang, R., Gan, X., Yang, X., Chen, L., & Jian, J. (2019). MicroRNA-384-5p/beclin-1 as potential indicators for epigallocatechin gallate against cardiomyocytes ischemia reperfusion injury by inhibiting autophagy via PI3K/Akt pathway. *Drug Design, Development and Therapy*, 13, 3607–3623. <https://doi.org/10.2147/DDDT.S219074>
- Zhang, J., Bai, K., Su, W., Wang, A., Zhang, L., Huang, K., & Wang, T. (2018). Curcumin attenuates heat-stress-induced oxidant damage by simultaneous activation of GSH-related antioxidant enzymes and Nrf2-mediated phase II detoxifying enzyme systems in broiler chickens. *Poultry Science*, 97(4), 1209–1219. <https://doi.org/10.3382/ps/pex408>
- Zhang, J., Ma, G., Guo, Z., Yu, Q., Han, L., Han, M., & Zhu, Y. (2018). Study on the apoptosis mediated by apoptosis-inducing-factor and influencing factors of bovine muscle during postmortem aging. *Food Chemistry*. <https://doi.org/10.1016/j.foodchem.2018.06.032>
- Zhang, J., Yu, Q., Han, L., Chen, C., Li, H., & Han, G. (2017). Study on the apoptosis mediated by cytochrome c and factors that affect the activation of bovine longissimus muscle during postmortem aging. *Apoptosis*, 22(6), 777–785. <https://doi.org/10.1007/s10495-017-1374-2>
- Zhang, J., Yu, Q., Han, L., Han, M., & Han, G. (2020). Effects of lysosomal iron involvement in the mechanism of mitochondrial apoptosis on postmortem muscle protein degradation. *Food Chemistry*, 127174. <https://doi.org/10.1016/j.foodchem.2020.127174>
- Zhao, F., Wang, X., Li, Y., Chen, X., Geng, Z., & Zhang, C. (2021). Effects of dietary supplementation with epigallocatechin gallate on meat quality and muscle antioxidant capacity of broilers subjected to acute heat stress. *Animals*, 11(11), 1–10. <https://doi.org/10.3390/ani11113296>
- Zhong, R., Li, H., Fang, Y., Sun, H., & Zhou, D. (2015). Effects of dietary supplementation with green tea polyphenols on digestion and meat quality in lambs infected with *Haemonchus contortus*. *Meat Science*, 105, 1–7. <https://doi.org/10.1016/j.meatsci.2015.02.003>